J Supercond Nov Magn (2015) 28:3027–3035
DOI 10.1007/s10948-015-3126-2

ORIGINAL PAPER

First-Principles Study of Magnetism and Half-Metallic Properties for the Quaternary Heusler Alloys CoMnTiZ (Z = P, As, and Sb)

M. Khodami[1] · F. Ahmadian[1]

Received: 30 March 2015 / Accepted: 15 May 2015 / Published online: 2 June 2015
© Springer Science+Business Media New York 2015

Abstract The ab initio calculations based on the density functional theory (DFT) using the self-consistent full-potential linearized augmented plane wave (FPLAPW) method were performed to study the electronic structure and magnetism of CoMnTiZ (Z = P, As, and Sb) quaternary Heusler compounds. The results showed that these compounds in the stable structure of Y_I were true half-metallic (HM) ferromagnets. The minority (half-metallic) band gaps were found to be 0.60 (0.27) 0.36 (0.16), and 0.43 (0.10) eV for Z = P, As, and Sb, respectively. The characteristic of energy bands and origin of minority band gaps were also studied. The total magnetic moments of CoMnTiZ (Z = P, As, and Sb) compounds were obtained 1 μ_B per formula unit, which were in agreement with Slater–Pauling rule ($M_{tot} = Z_{tot} - 24$). The CoMnTiZ (Z = P, As, and Sb) compounds maintained the HM character at ranges of 5.43–5.91, 5.44–5.89, and 5.46–6.22Å, respectively, which makes them ideal candidates for spintronic applications.

Keywords Half-metals · Quaternary Heusler alloys · Magnetic properties · Electronic properties

✉ F. Ahmadian
farzad.ahmadian@gmail.com; ahmadian@iaush.ac.ir

[1] Department of Physics, Shahreza Branch, Islamic Azad University, Shahreza, Iran

1 Introduction

Spintronics is one of the most important and practical fields in science. The injection of a spin-polarized current from a ferromagnet to a semiconductor is necessary for the spintronic devices [1]. Half-metallic (HM) ferromagnets are promising candidates in spintronic industry, in which one of the two spin channels is metallic and the other is semiconducting or insulating. This leads to 100 % spin polarization at the Fermi level. The first predicted HM material was the NiMnSb half-Heusler alloy found by de Groot et al. in 1983 [2]. HM characteristics have been predicted in several materials, such as ferromagnetic metallic oxides [3–5], dilute magnetic semiconductors [6, 7], zincblende transition-metal pnictides and chalcogenides [8–12], *sp* compounds (without transition metals) with zinc-blende and rocksalt structures such as CaC, SrN, and RbX (X = Sb, Te) [13–15], and Heusler alloys, e.g., Co_2MnSi [16] and Mn_2ZnCa [17].

Among the HM materials, the Heusler alloys have attracted great interests due to their easy synthesis and high Curie temperature [18–24]. Heusler alloys have the structural formulas of X_2YZ with $L2_1$ structure and XYZ with C_{1b} structure, where X and Y are transition metals and Z is a main-group element. There are some theoretical studies which predicted HM characteristic in Heusler compounds mainly in Co_2-based alloys with $L2_1$ structure [25–31].

Recently, many efforts have been made to investigate the quaternary Heusler alloys XX′YZ (X, X′, and Y are transition metals, and Z is a main-group element) instead of the ternary ones (X_2YZ and XYZ). In these compounds, the valence of X′ is lower than the valence of X atoms, and the valence of the Y element is lower than the valence of both X and X′. XX′YZ quaternary Heusler compounds crystallize

in the LiMgPdSn-type crystal structure [32, 33] with $F\bar{4}3m$ symmetry.

Ni-based quaternary Heusler ferromagnets, NiFeMnGa and NiCoMnGa, with high spin polarization have been studied recently [34]. The pseudopotential calculations on the electronic structure, elastic, and magnetic properties of NiCoCrGa quaternary Heusler compound showed that this compound was a typical half-metal with very high spin polarization at the Fermi level [35]. Gao et al. [36] have used the first-principles calculations to design new quaternary Heusler compounds of CoFeCrZ (Z = Ga, Ge, Al, and Si). They showed that both CoFeCrGa and CoFeCrGe were nearly half-metals, while both CoFeCrAl and CoFeCrSi exhibited excellent HM ferromagnetism. Xiong et al. [37] investigated the electronic structure and magnetic properties of 12 quaternary Heusler alloys CoFeTiZ and CoFeVZ (Z = Al, Ga, Si, Ge, As, and Sb) using the first-principles calculations. Their calculations showed that CoFeTiSi, CoFeTiAs, and CoFeVSb were HM ferromagnets, CoFeTiAl and CoFeTiGa were conventional semiconductors, and other alloys were nearly half-metal. Recently, the first-principle calculations were performed on CoFeTiSb quaternary compound by Berri et al. [38] who introduced this compound as a stable HM ferrimagnetism. Afterwards, Berri et al. [39] also studied the electronic and magnetic properties of the ZrFeTiAl, ZrFeTiSi, ZrFeTiGe, and ZrNiTiAl quaternary Heusler compounds and predicted that these compounds were HM ferromagnets.

However, there are few studies on quaternary Heusler systems; therefore, it is interesting to investigate these new HM materials theoretically. To the best of our knowledge, there is no detailed experimental or theoretical investigation on CoMnTiZ (Z = P, As, and Sb) quaternary alloys. In this study, we intent to design the new quaternary Heusler compounds CoMnTiZ (Z = P, As, and Sb) using first-principles density functional calculations.

2 Computational Method

Present calculations were performed applying the first-principles full-potential linearized augmented plane wave (FPLAPW) method to the density functional theory (DFT) implemented with the Wien2k package [40]. In this method, the space of unit cell is divided into non-overlapping muffin-tin (*MT*) spheres which are separated by an interstitial region. Kohn–Sham wave functions are expanded in terms of spherical harmonic functions inside muffin-tin spheres and expanded terms of Fourier series in the interstitial region. The plane wave cutoff ($K_{\max}$) was chosen as $8.0/R_{\mathrm{MT}}$ for the expansion of the wave functions in the interstitial region. For the wave function expansion inside muffin-tin spheres, the maximum value of the orbital momentum ($l_{\max}$) was assumed equal to 10. The Co, Mn, Ti, and Z (=P, As, and Sb) muffin-tin sphere radii were chosen 2.0 Bohr. The exchange-correlation potential was calculated using the generalized gradient approximation based on Perdew, Burke, and Ernzerhof scheme (PBE-GGA) [41]. The charge density and potential function in the interstitial region were expanded up to $G_{\max} = 12(Ryd)^{1/2}$. A mesh of 84 special k-points was made in the irreducible wedge of the Brillouin zone. The self-consistent calculations converge only when the integrated charge difference per formula unit $[\int |\rho_n - \rho_{n-1}|\, dr]$ between the input charge density $\left[\rho_{n-1}(r)\right]$ and the output charge density $[\rho_n(r)]$ is less than 0.00001.

3 Results and Discussion

3.1 Structural Properties

The quaternary Heusler compounds in the LiMgPdSn-type crystal structure have three possible structures of Y_{I}, Y_{II}, and Y_{III}. For the Y_{I} structure of CoMnTiZ compounds, the Wyckoff positions of 4*a* (0, 0, 0), 4*b* (1/2 1/2 1/2), 4*c* (1/4, 1/4, 1/4), and 4*d* (3/4, 3/4, 3/4) were occupied by Co, Mn, Ti and Z atom, respectively. The crystal structure of CoMnTiP compound in the Y_{I} structure is shown in Fig. 1. The $Y_{\mathrm{II}}/Y_{\mathrm{III}}$ structure is formed by placing Co, Mn, Ti and Z at (4*a*, 4*d*, 4*b* and 4*c*)/(4*a*, 4*d*, 4*c* and 4*b*), respectively. In order to obtain the true ground state of CoMnTiZ (Z = P, As, and

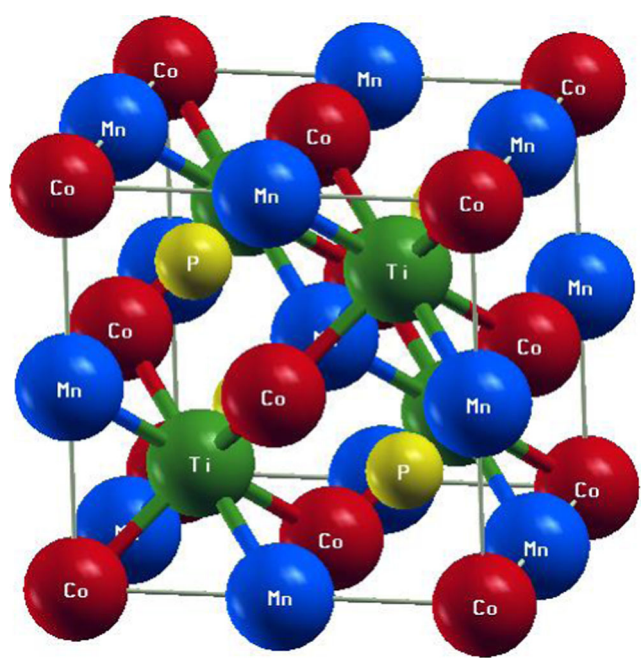

Fig. 1 Crystal structure of CoMnTiP quaternary Heusler compound in the Y_{I} structure

Sb), the structural optimization was performed by minimizing of energy as a function of unit cell volume for the three structures. The calculated total energies versus unit cell volume were fitted to the Murnaghan equation of state [42]. The total energy versus volume for the three structures was shown in Fig. 2. Accordingly, the Y_I structure has the lowest energy among three structures making it the ground state structure for all compounds. Hence, all the further results only focus on this structure.

The equilibrium structural parameters including the lattice parameter, bulk modulus and derivative of bulk modulus are listed in Table 1 for CoMnTiZ (Z = P, As, and Sb) compounds. There is a good agreement between the calculated lattice parameter of CoMnTiAs with the only available value (5.83 Å) reported by Özdoğan et al. [43].

The cohesive energy (E_C) of a solid is defined as the energy required for separating the condensed material into isolated free atoms. The cohesive energy of CoMnTiZ compounds per formula unit is obtained from the following relation:

$$E_C^{CoMnTiZ} = E_{tot}^{CoMnTiZ} - (E_{Co} + E_{Mn} + E_{Ti} + E_Z); \quad (Z = P, \text{As, and Sb}) \tag{1}$$

where $E_{tot}^{CoMnTiZ}$ is the equilibrium total energy of the CoMnTiZ compounds, and E_{Co}, E_{Mn}, E_{Ti}, and E_Z are the total energies of the pure atomic components. The estimated values of cohesive energy (Table 1) guarantee the structural stability of CoMnTiZ Heusler compounds in the Y_I structure.

The formation energies (E_f) were also calculated for CoMnTiZ Heusler compounds by subtracting the equilibrium total energies with bulk energies of Co, Mn Ti, and Z as

$$E_f^{CoMnTiZ} = E_{tot}^{CoMnTiZ} - \left(E_{Co}^{bulk} + E_{Mn}^{bulk} + E_{Ti}^{bulk} + E_Z^{bulk}\right) \tag{2}$$

The negative values of E_f for the CoMnTiZ compounds (Table 1) show that these compounds are stable in both structures and can be synthesized experimentally

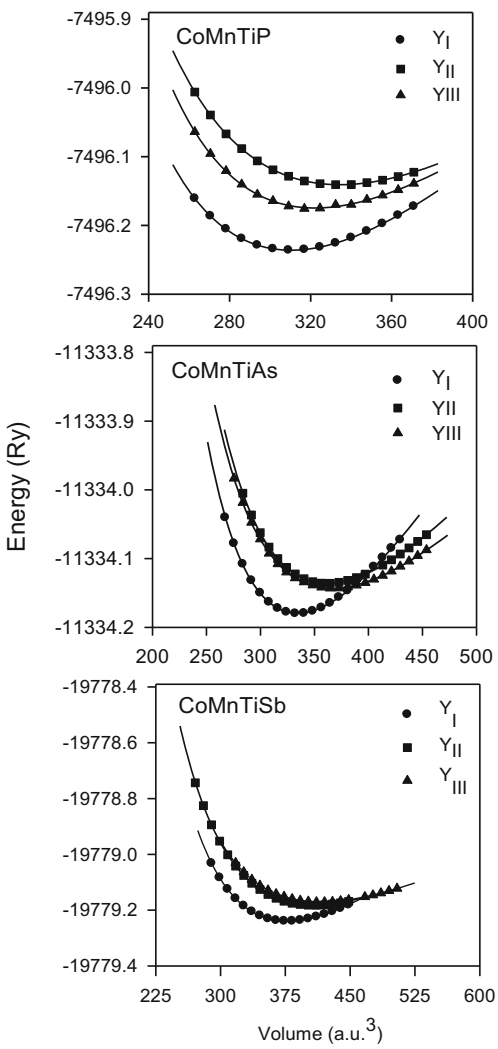

Fig. 2 Total energy as a function of unit cell volume for the CoMnTiZ (Z = P, As, and Sb) compounds in the Y_I, Y_{II}, and Y_{III} structures

3.2 Electronic Properties

The calculated spin-polarized band structures of CoMnTiZ (Z = P, As, and Sb) compounds at the equilibrium lattice constant along high-symmetry directions of the first Brillouin zone were displayed in Fig. 3. Accordingly, for all compounds, the Fermi level crosses energy bands in spin-up (majority spin) state and the band structure shows a metallic characteristic, while in the spin-down (minority spin) state, the Fermi level is located within band gap and the band structure shows a semiconducting nature. Therefore, there is a 100 % spin polarization at the Fermi level and CoMnTiZ compounds are HM ferromagnets at the equilibrium lattice constant.

In order to get more information about the characteristic of the energy bands around the Fermi level, the band structure of CoMnTiZ compounds was investigated in detail. In the usual XX′YZ Heusler compounds, the Z atoms offers a single *s* and a triple-degenerated *p* band per spin direction which are located at low energy levels (below the *d* bands). These bands are important since they accommodate charge from the transition-metal atoms which reduces the effective *d* charge and stabilizes the structure. According to Fig. 3, the three energy bands between −8 and −4 eV belong to Z *p* states, and the single band, which is isolated from other bands and located at lower energies, is relative to Z *s* states. Concerning the hybridization between the *d* orbitals of the transition-metal atoms, the X–X′ interactions should be considered at first. The *d* orbitals of the X and

Table 1 The calculated bulk parameters of CoMnTiZ (Z = P, As, and Sb) compounds in Y_{I}, Y_{II}, and Y_{III} structures

Compound	Structure	a (Å)	B (Gpa)	B_0	E_{c} (Ry)	E_{f} (Ry)
CoMnTiP	YI	5.69	220.10	4.75	−1.46	−0.20
	YII	5.83	162.95	4.48	−1.37	−0.10
	YIII	5.76	190.30	5.31	−1.40	−0.13
CoMnTiAs	YI	5.83	190.20	5.03	−1.38	−0.13
	YII	5.99	136.88	4.88	−1.33	−0.08
	YIII	6.02	116.30	4.83	−1.37	−0.09
CoMnTiSb	YI	6.07	177.85	4.44	−1.46	−0.21
	YII	6.61	131.59	4.14	−1.04	−0.16
	YIII	6.26	105.08	4.56	−1.39	−0.14

a(Å) lattice parameter, B(GPa) bulk module, B_0 derivative of bulk module, E_{c} (Ry) cohesive energy, E_{f}(Ry) formation energy

X′ atoms hybridize strongly creating five bonding d hybrids (the double-degenerated e_g and the triple-degeneratedt_{2g} hybrids which obey the tetrahedral symmetry) and five non-bonding d states (the double-degenerated e_u states and the triple-degenerated t_{1u} states which have octahedral symmetry). Due to similar symmetry of bonding d hybrids and d orbitals of the Y atom (with tetrahedral symmetry), they can hybridize and create five bonding and five antibonding hybrids. The five non-bonding d states, which have octahedral symmetry, cannot couple with the d orbitals of the Y atoms with tetrahedral symmetry (a schematic representation of the d–d hybridizations in the XX′YZ Heusler compounds is shown in Fig. 4). This mechanism is observed in Fig. 3 for CoMnTiZ (Z = P, As, and Sb) compounds. For example, the energy bands in spin minority state between −4 and −2.5 eV are mainly relative to five bonding states for CoMnTiP compound. The three bands between −2.5 and 0 eV belong to the triple-degenerated t_{1u} states. There is an energy gap between the non-bonding occupied t_{1u} and the unoccupied e_u states. The non-bonding e_u states and the anti-bonding e_g and t_{2g} states are above the Fermi level from 0 to 5 eV.

Comparing the p bands of CoMnTiZ compounds (Fig. 3) shows that the p states of CoMnTiP have lower energies relative to the Fermi level than those of CoMnTiAs. Therefore, the p states of CoMnTiAs were pushed to higher energies. Besides, the p bands of CoMnTiSb were higher than those of CoMnTiAs due to the higher energy of their p states than those of CoMnTiAs. In fact, with increasing the valence electrons of Z atoms (P → As → Sb), the energy of the p states of these atoms increase and p bands shift toward higher energies.

The minority-spin band gap (E_g), which is determined by subtracting the energies of the highest occupied and the lowest unoccupied bands in the minority-spin state and HM gap (E_{HM}), is defined as the minimum energy required to flip a minority-spin electron from the valance band maximum to the majority-spin Fermi level are listed in Table 2 for CoMnTiZ (Z = P, As, and Sb) Heusler compounds. The existence of a non-zero spin-flip gap in the three compounds shows that they are true HM ferromagnets. Among three compounds, the largest values of E_g and E_{HM} belong to CoMnTiP. According to Table 2, as the valence electrons of Z atom increase (along P → As → Sb sequence), the E_{HM} values decrease In fact, the difference between the electronic configurations of the Z elements may influence the position of the Fermi level and the size of the band gap.

To investigate the origin of minority band gap in the CoMnTiZ (Z = P, As, and Sb) compounds, the total and orbital density of states (DOSs) for CoMnTiP are presented in Fig. 5 as representative of all compounds. Accordingly, there was a strong hybridization between Co, Mn, and Ti atoms, which splits the d orbitals of these atoms into bonding $e_g$and t_{2g}orbitals (below the Fermi level), non-bonding $e_{\mathrm{u}}$and t_{1u}orbitals (around the Fermi level), and anti-bonding $e_g$and t_{2g}orbitals (above the Fermi level). This hybridization puts the Fermi level in the minority band gap. In fact, d–d hybridization between transition metals takes part in the formation of minority band gap known as d–d band gap The d–d band gap was the origin of the HM band gap in the full-Heusler alloys with $AlCu_2Mn$ structure [44]. Moreover the bonding states mainly belong to the high-valent transition metal atom Co. In contrast, while the unoccupied antibonding states were mainly at the low-valent transition metal atom Ti, which indicates the covalent hybridization between high-valent and low-valent atoms, leading to the appearance of minority-spin energy gap. The covalent band gap exists in the half-Heusler compounds with C_{1b} structure [44]. Both$d$–d and covalent band gaps have been recently observed in inverse Heusler compounds such as Ti_2CoSn [45] and Sc_2MnZ (Z = C, Si, Ge, and Sn) [46]. A weaker hybridization is also observed between d states of Co, Mn, and Ti atoms with p states of P atom, which determine the

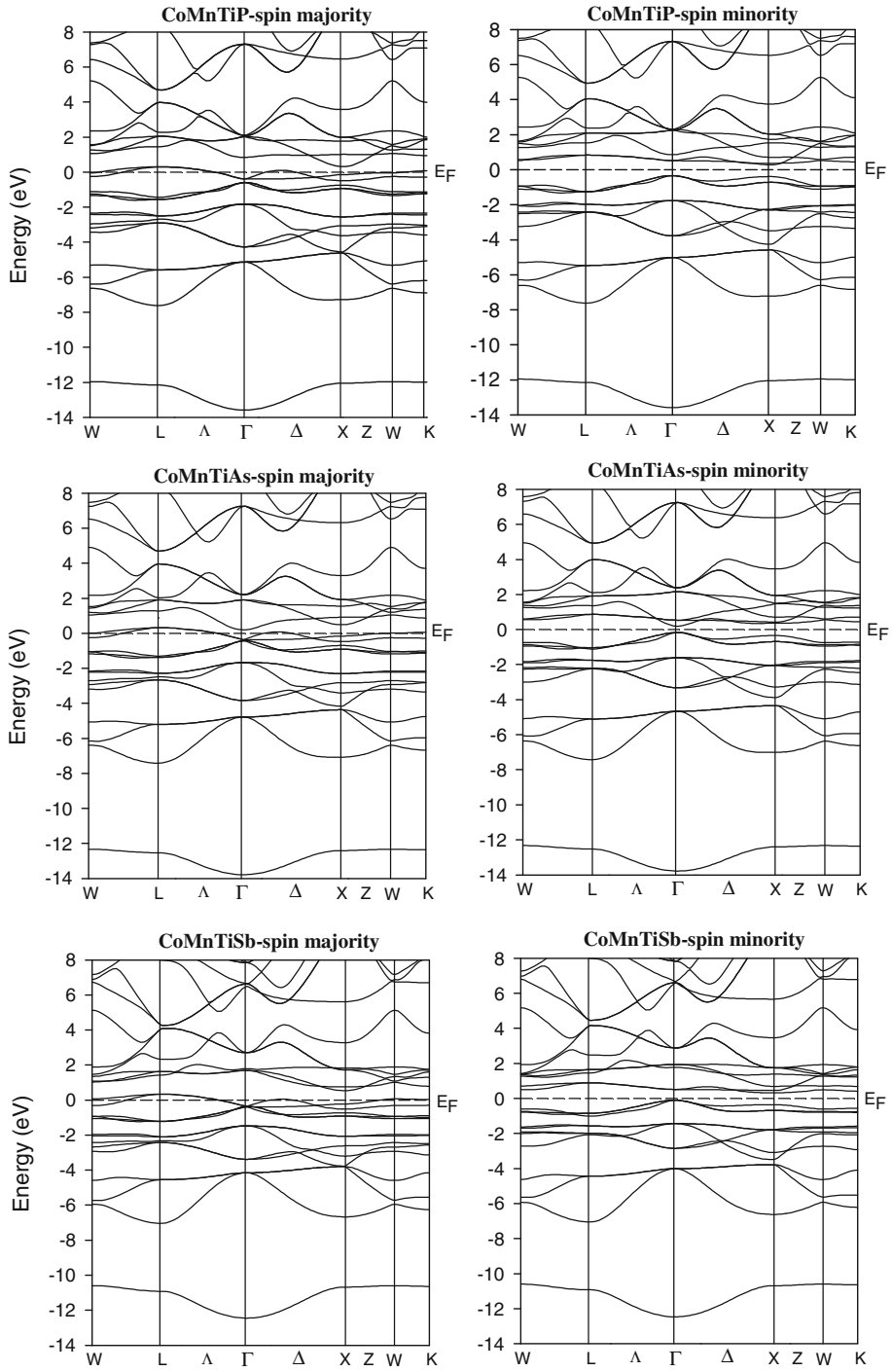

Fig. 3 The band structures of CoMnTiZ(Z = P, As, and Sb) compounds at the equilibrium lattice parameter. The dash line at 0 eV indicates the Fermi energy (E_F)

degree of occupation of the *p–d* orbital. This hybridization affects the width of energy gap.

3.3 The Effect of the Lattice Parameter on Half-Metallicity

In order to study the effect of lattice constant on the band gap and the stability of the HM property, it was necessary to investigate the influence of the compression and expansion stress on the band gap by changing the lattice constant of the compounds. The values of the minority band gaps versus lattice constants are plotted for CoMnTiZ (Z = P, As, and Sb) compounds in Fig. 6 Accordingly the CoMnTiP, CoMnTiAs, and CoMnTiSb compounds were respectively half-metals in the range of 5.43–5.91, 5.44–5.89 and 5.46–6.22 Å. Among these compounds the CoMnTiSb has a

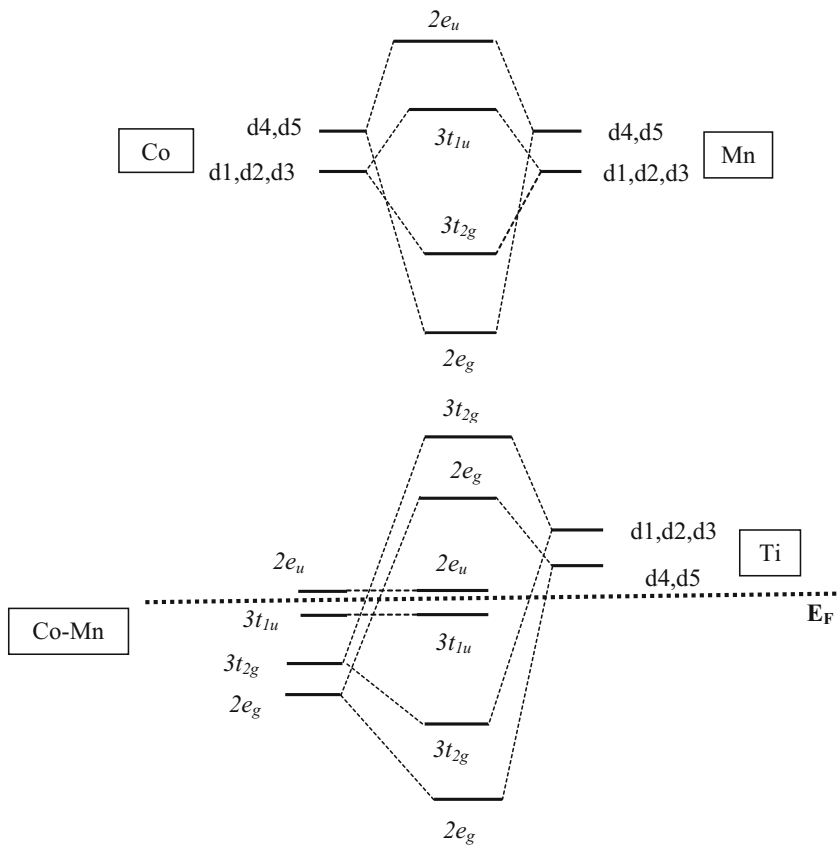

Fig. 4 A schematic representation of the *d*-*d* hybridizations between spin-down orbitals of transition metals sitting at different sites for the CoMnTiZ quaternary Heusler compounds

considerable region of half-metallicity which makes it stable against negative and positive pressures. Moreover, in the CoMnTiP, the Fermi level was located in the middle of the minority band gap and therefore, this compound is the most stable compound against the effects which destroy the half-metallicity (such as temperature or quasi-particle excitations). A common behavior in the CoMnTiP and CoMnTiAs compounds is observed that with increasing the lattice constant, the minority valence band edge smoothly changes, while the minority conduction band edge initially increases and subsequently shifts quickly toward the Fermi level. In both compounds, for high and low lattice constants the minority conduction band edge crosses the Fermi level and destroys the half-metallicity. There is a different behavior in the CoMnTiSb, that with increasing the lattice constant, the minority valence band edge smoothly increases and subsequently cuts the Fermi level, while with decreasing the lattice constant the minority conduction band edge smoothly decreases and disappears the half-metallicity. Galanakis et al. [47] showed that the contraction and expansion of the lattice constant mainly influence the delocalized *p*electrons and do not affect the well localized *d* electrons of the transition metals considerably.

3.4 Magnetic Properties

The total and atomic magnetic moments of CoMnTiZ (Z = P, As, and Sb) compounds are listed in Table 3. Accordingly, the total magnetic moment (M_{tot}) of CoMnTiZ compounds was an integer value of 1 μ_B. The integer total magnetic moment (M_{tot}) is a typical characteristic of HM ferromagnets. The M_{tot} of HM materials usually follows Slater–Pauling (SP) law. To find the proper SP rule for CoMnTiZ compounds, the minority-spin band structure of each compound should be considered According to Fig. 3 the minority-spin bands of CoMnTiZ compounds were occupied by a total of 12 electrons per unit cell: one

Table 2 The calculated minority-spin (E_g) and half-metallic (E_{HM}) band gaps of CoMnTiZ (Z = P, As, and Sb) compounds at equilibrium lattice constant

Compound	E_g (eV)	E_{HM}(eV)
CoMnTiP	0.60	0.27
CoMnTiAs	0.36	0.16
CoMnTiSb	0.43	0.10

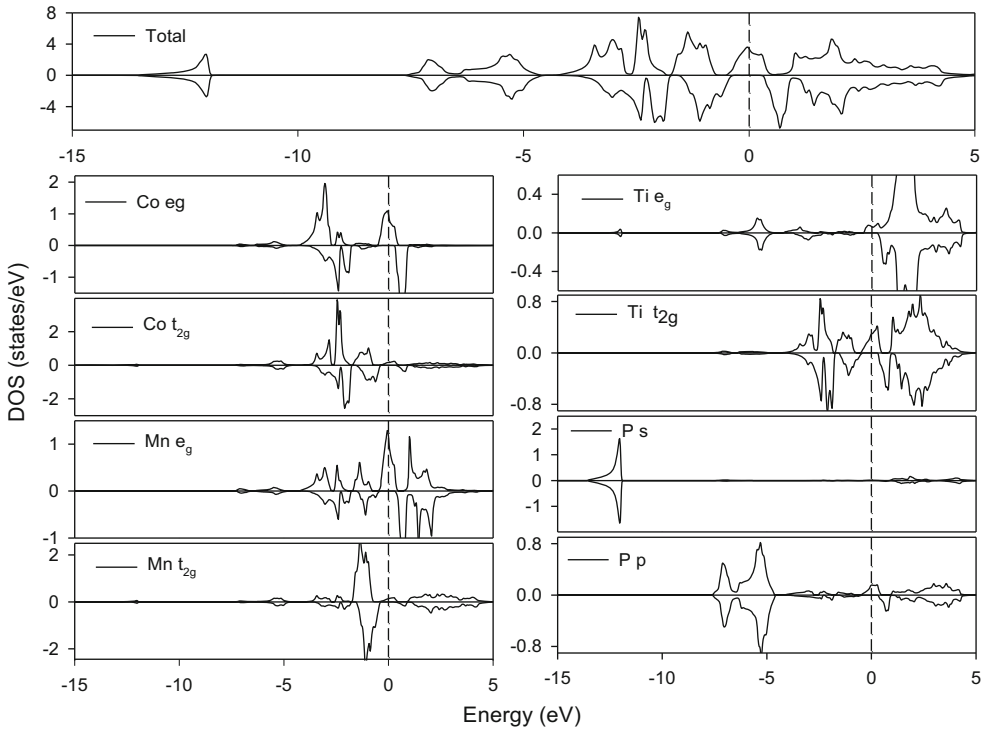

Fig. 5 The calculated total and partial DOSs for the CoMnTiP compound. Positive values of DOS are chosen as majority spin electrons and negative values as minority ones. The zero energy value corresponds to the Fermi level

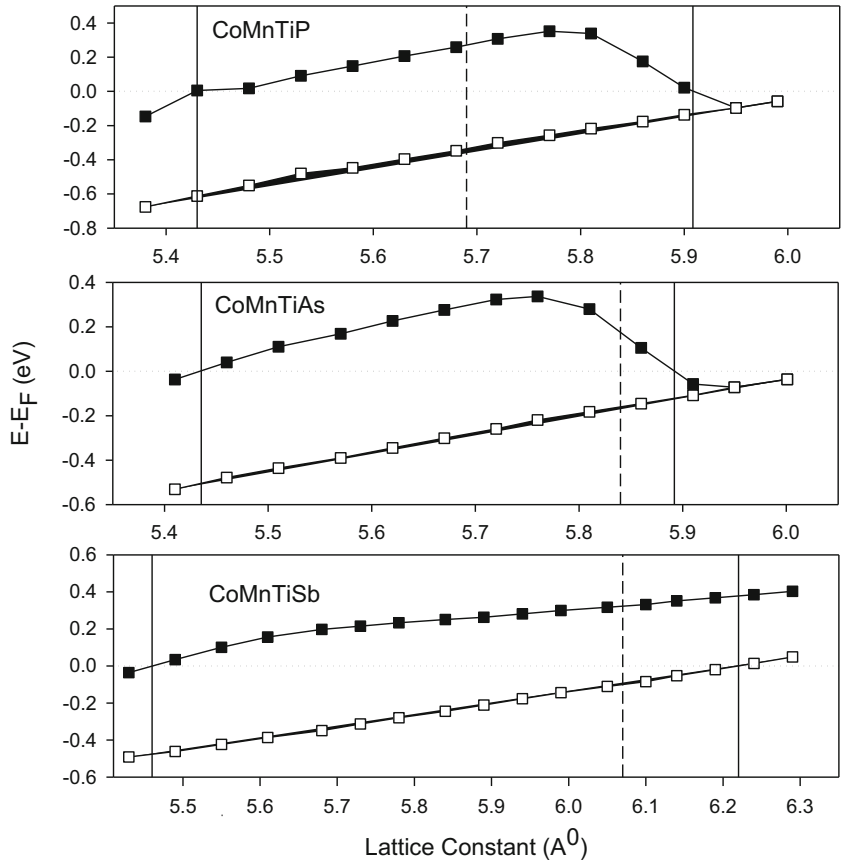

Fig. 6 The minority band gap of CoMnTiZ (Z = P, As, and Sb) compounds as a function of the lattice constant. The *white* and *black squares* show the valence band minimum (VBM) and conduction band maximum (CBM), respectively. The *vertical dashed line* indicates the equilibrium lattice constant, and *vertical solid lines* show the range of half-metallicity. The *horizontal dotted line* at 0 eV shows the Fermi energy

Table 3 The total and atomic magnetic moments of CoMnTiZ (Z = P, As, and Sb) compounds

Compound	M_{tot}	M_{Co}	M_{Mn}	M_{Ti}	M_Z	M_{Int}
CoMnTiP	1.00	0.67	0.43	−0.06	0.006	−0.05
CoMnTiAs	1.00	0.66	0.48	−0.08	0.003	−0.07
CoMnTiSb	1.00	0.67	0.53	−0.10	0.005	−0.09

M_{tot} (μ_B) total magnetic moment, M_{Co} (μ_B) Co magnetic moment, M_{Mn} (μ_B) Mn magnetic moment, M_{Ti} (μ_B) Ti magnetic moment, M_Z (μ_B) Z magnetic moment, M_{Int} (μ_B) magnetic moment in the interstitial region

with a s character, three with a p character, five bonding d hybrids (e_g and t_{2g} hybrids), and two non-bonding d states (e_u states). Thus, the number of occupied spin-up states ($N\uparrow$) is calculated as

$$N\uparrow = Z_{tot} - N\downarrow = Z_{tot} - 12 \tag{3}$$

where $N\downarrow$ is the number of occupied spin-down states and the M_{tot} is

$$\begin{aligned} M_{tot} &= (N\uparrow - N\downarrow)\mu_B = (Z_{tot} - 2N\downarrow)\mu_B \\ &= (Z_{tot} - 24)\mu_B \end{aligned} \tag{4}$$

The CoMnTiZ (Z = P, As, and Sb) compounds have 25 valence electrons. Therefore, M_{tot} of these compounds satisfy Eq. 4. The M_{tot} contain five contributions from the Co atom, the Mn atom, the Ti atom, the Z atom, and the interstitial region. Table 3 shows that the main contribution to the M_{tot} comes from the Co and Mn atoms. The Co and Mn atoms have positive magnetic moments, while Ti atom has a negative magnetic moment. The magnetic moment of Z atom is very small. As a result, the atoms in the CoMnTiZ (Z = P, As, and Sb) compounds are in ferrimagnetic arrangement.

The total and atomic magnetic moments of CoMnTiZ (Z = P, As, and Sb) compounds as functions of the lattice constant are also calculated and presented in Fig. 7. As can be seen, for CoMnTiP compound, the M_{tot} was 1 μ_B integer value in a relatively wide range of lattice parameters (about 0.5 Å), but by applying positive and negative pressures on lattice, the M_{tot} decreases to values below 1 μ_B In CoMnTiAs and CoMnTiSb compounds, the M_{tot} was an integer value for a wider range of lattice parameters. However, for the three compounds, the partial spin moments of Co, Mn, Ti, and Z atoms were quite sensitive to the lattice distortion. The absolute values of the moment of Co and Mn atoms (with positive sign) increase with increasing lattice constant, while the partial moment of Ti decreases with the expansion of the lattice constant to achieve a constant M_{tot} in the unit cell. With expanding the lattice constant, the hybridization between neighboring atoms may decrease and their atomic-like character increases which leads to an enhancement in their spin moments. This behavior was also observed in several Heusler alloys [48].

4 Conclusion

The electronic structure and magnetism of the CoMnTiZ (Z = P, As, and Sb) quaternary Heusler compounds were investigated using FPLAPW method. The results showed

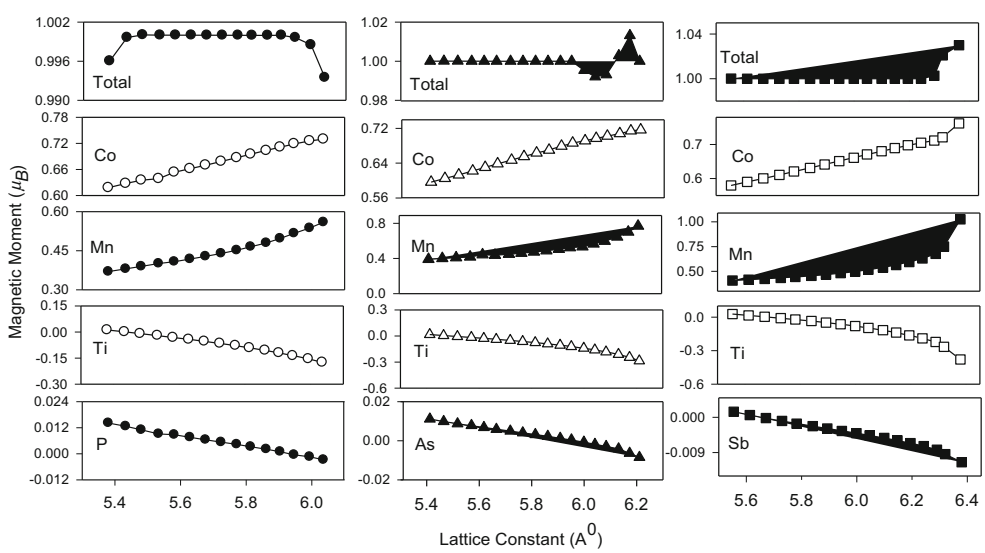

Fig. 7 Total and atomic magnetic moments as functions of the lattice constant for the CoMnTiZ (Z = P, As, and Sb) compounds

that all compounds in stable Y_I structure have HM characteristic. The HM band gaps were mainly determined from the hybridizations of the d states between Co, Mn, and Ti atoms The sensitivity of the half-metallicity was analyzed under uniform distortion. The halfmetallicity was robust for lattice constants range of 5.43–5.91, 5.44–5.89 and 5.46–6.22 for Z elements of P, As, and Sb, respectively. The M_{tot} of CoMnTiZ compounds was found to be an integer value of 1 μ_B which was in agreement with the Slater–Pauling rule ($M_{tot} = Z_{tot} - 24$). The stability of HM character of CoMnTiZ compounds against relatively large uniform strains would make them promising materials for future spintronic applications.

References

1. Žutic, I., Fabian, J., Das Sarma, S.: Rev. Mod. Phys. **76**, 323 (2004)
2. de Groot, R.A., Mueller, F.M., van Engen, P.G., Buschow, K.H.J.: Phys. Rev. Lett. **50**, 2024 (1983)
3. Szotek, Z., Temmerman, W.M., Svane, A., Petit, L., Stocks, G.M., Winter, H.: J. Magn. Magn. Mater., 2721816 (2004)
4. Song, W., Wang, J., Wu, Z.: Chem. Phys. Lett. **482**, 246 (2009)
5. Lv, S., Li, H., Han, D., Wu, Z., Liu, X., Meng, J.: J. Magn. Magn. Mater. **323**, 416 (2011)
6. Zhang, Y., Liu, W., Niu, H.: Solid State Commun. **145**, 590 (2008)
7. Saeed, Y., Nazir, S., Shaukat, A., Reshak, A.H.: J. Magn. Magn. Mater. **322**, 3214 (2011)
8. Galanakis, I., Mavropoulos, P.: Phys. Rev. B **67**, 104417 (2003)
9. Xu, Y.-Q., Liu, B.-G., Pettifor, D.G.: Physica B **1117**, 329–333 (2003)
10. Yao, K.L., Gao, G.Y., Liu, Z.L., Zhu, L.: Solid State Commun. **133**, 301 (2005)
11. Yao, K.L., Gao, G.Y., Liu, Z.L., Zhu, L., Li, Y.L.: Physica B **366**, 62 (2005)
12. Ge, X.-F., Zhang, Y.-M.: J. Magn. Magn. Mater. **321**, 198 (2009)
13. Gao, G.Y., Yao, K.L., Şaşıoğlu, E., Sandratskii, L.M., Liu, Z.L., Jiang, J.L.: Phys. Rev. B **75**, 174442 (2007)
14. Geshi, M., Kusakabe, K., Nagara, H., Suzuki, N.: Phys. Rev. B **76**, 054433 (2007)
15. Şenol, Ç., Kervan, S., Kervan, N.: Intermetallics **52**, 1 (2014)
16. Nourmohammadi, A., Abolhasani, M.R.: Solid. State. Commun. **150**, 1501 (2010)
17. Wang, W.Z., Wei, X.P.: Comput. Mater. Sci. **50**, 2253 (2011)
18. Felser, C., Fecher, G.H., Balke, B.: Angew. Chem. Int. Ed. **46**, 668 (2007)
19. Graf, T., Felsler, C., Parkin, S.P.P.: Prog. Solid State Chem. **39**, 1 (2011)
20. Saito, T. et al.: Phys. Rev. B **81**, 144417 (2010)
21. Farshchi, R., Ramsteiner, M.: J. Appl. Phys. **113**, 191101 (2013)
22. Wei, X.-P., Deng, J.-B., Mao, G.-Y., Chu, S.-B., Hu, X.-R.: Intermetallics **29**, 86 (2012)
23. Kervan, N., Kervan, S.: J. Magn. Magn. Mater. **324**, 645 (2012)
24. Kervan, N.: J. Magn. Magn. Mater. **324**, 4114 (2012)
25. Chen, X.-Q., Podloucky, R., Rogl, P.: J. Appl. Phys. **100**, 113901 (2006)
26. Özdoğan, K., Galanakis, I., Şasıoğlu, E., Aktaş, B.: Solid State Commun **142**, 492 (2007)
27. Kandpal, H.C., Fecher, G.H., Felser, C.: J. Phys. D: Appl. Phys. **40**, 1507 (2007)
28. Liu, G.D., Dai, X.F., Lui, H.Y., Chen, J.L., Li, Y.X., Xiao, G., Wu, G.H.: Phys. Rev. B **77**, 14424 (2008)
29. Özdoğan, K., Galanakis, I.: J. Magn. Magn. Mater. **321**, L34 (2009)
30. Sharma, V., Solanki, A.K., Kashyap, A.: J. Magn. Magn. Mater. **322**, 2922 (2010)
31. Mori, H., Odahara, Y., Shigyo, D., Yoshitake, T., Miyoshi, E.: Thin Solid Films **520**, 4979 (2012)
32. Dai, X., Liu, G., Fecher, G.H., Felser, C., Li, Y., Liu, H.: J. Appl. Phys. **105**, 07E901 (2009)
33. Xu, G.Z., Liu, E.K., Du, Y., Li, G.J., Liu, G.D., Wang, W.H., Wu, G.H.: EPL **102**, 17007 (2013)
34. Alijani, V., Winterlik, J., Fecher, G.H., Naghavi, S.S., Felser, C.: Phys. Rev. B **184428**, 83 (2011)
35. Gökoğlu, G.: Solid. State. Sci. **14**, 1273 (2012)
36. Gao, G.Y., Hu, L., Yao, K.L., Luo, B., Liu, N. J. Alloy. Compd. **551**, 539 (2013)
37. Xiong, L., Yi, L., Gao, G.Y.: J. Magn. Magn. Mater. **360**, 98 (2014)
38. Berri, S., Maouche, D., Ibrir, M., Zerarga, F.: J. Magn. Magn. Mater. **354**, 65 (2014)
39. Berri, S., Ibrir, M., Maouche, D., Attallah, M.: J. Magn. Magn. Mater. **371**, 106 (2014)
40. Blaha, P., Schwarz, K., Madsen, G.K.H., Hvasnicka, D., Luitz, J.: WIEN2k, an augmented plane wave ? local orbitals program for calculating crystal properties. Technische Universit Wien, Austria, Karlheinz Schwarz (2001). ISBN 3-9501031-1-2
41. Perdew, J., Burke, K., Ernzerhof, M.: Phys. Rev. Lett. **77**, 3865 (1996)
42. Murnaghan, F.D.: Proc. Natl. Acad. Sci. U.S.A. **30**, 244 (1947)
43. Özdoğan, K., Şasıoğlu, E., Galanakis, I.: J. Appl. Phys. **113**, 193903 (2013)
44. Wei, X.-P., Deng, J.-B., Mao, G.-Y., Chu, S.-B., Hu, X.-R.: Intermetallics **29**, 86 (2012)
45. F.Ahmadian: J. Alloy. Compd. **576**, 279 (2013)
46. Ahamdian, F., Salary, A.: Intermetallics **46**, 243 (2014)
47. Galanakis, I., Özdoğan, K., Şasıoğlu, E.: J. Phys.: Condens. Matter **26**, 086003 (2014)
48. Galanakis, I., Mavropoulos, Ph., Dederichs, P.H.: J. Phys. D: Appl. Phys. **39**, 765 (2006)